Hindawi Publishing Corporation
International Journal of Photoenergy
Volume 2011, Article ID 204639, 8 pages
doi:10.1155/2011/204639

Research Article

Synthesis and Application of New Ruthenium Complexes Containing β-Diketonato Ligands as Sensitizers for Nanocrystalline TiO_2 Solar Cells

Ashraful Islam,[1,2,3] Surya Prakash Singh,[1,2] and Liyuan Han[1,2]

[1] *International Center for Materials Nanoarchitectonics (MANA), National Institute for Materials Science (NIMS), 1-2-1 Sengen, Tsukuba, Ibaraki 305-0047, Japan*
[2] *Advanced Photovoltaics Center, National Institute for Materials Science (NIMS), 1-2-1 Sengen, Tsukuba, Ibaraki 305-0047, Japan*
[3] *Center of Excellence for Research in Engineering Materials (CEREM), College of Engineering, King Saud University, Riyadh 11421, Saudi Arabia*

Correspondence should be addressed to Ashraful Islam, islam.ashraful@nims.go.jp

Received 30 March 2011; Accepted 4 May 2011

Academic Editor: Mohamed Sabry Abdel-Mottaleb

Five heteroleptic ruthenium complexes having different β-diketonato ligands, [Ru(tctpy)(dppd)(NCS)] (**1**), [Ru(tctpy)(pd)(NCS)] (**2**), [Ru(tctpy)(tdd)(NCS)] (**3**), [Ru(tctpy)(mepd)(NCS)] (**4**), and [Ru(tctpy)(tmhd)(NCS)] (**5**), where tctpy = 4,4′,4″-tricarboxy-2,2′:6′,2″-terpyridine, pd = pentane-2,4-dione, mepd = 3-methylpentane-2,4-dione, tmhd = 2,2,6,6-tetramethylheptane-3,5-dione, tdd = tridecane-6,8-dione, and dppd = 1,3-diphenylpropane-1,3-dione, were synthesized and characterized. These heteroleptic complexes exhibit a broad metal-to-ligand charge transfer absorption band over the whole visible range extending up to 950 nm. The low-energy absorption bands and the $E(Ru^{3+/2+})$ oxidation potentials in these complexes could be tuned to about 15 nm and 110 mV, respectively, by choosing appropriate β-diketonate ligands. Molecular orbital calculation of complex **1** shows that the HOMO is localized on the NCS ligand and the LUMO is localized on the tctpy ligand, which is anchored to the TiO_2 nanoparticles. The β-diketonato-ruthenium(II)-polypyridyl sensitizers, when anchored to nanocrystalline TiO_2 films for light to electrical energy conversion in regenerative photoelectrochemical cells, achieve efficient sensitization to TiO_2 electrodes with increasing activity in the order **5** < **4** < **3** ≈ **2** < **1**. Under standard AM 1.5 sunlight, the complex **1** yielded a short-circuit photocurrent density of 16.7 mA/cm^2, an open-circuit voltage of 0.58 V, and a fill factor of 0.64, corresponding to an overall conversion efficiency of 6.2%. A systematic tuning of HOMO energy level shows that an efficient sensitizer should possess a ground-state redox potential value of > +.53 V versus SCE.

1. Introduction

Dye-sensitized solar cells (DSCs) have attracted a great deal of attention as one of the promising solar-to-electricity power conversion devices because of their high efficiency and their potential of low-cost production [1–6]. The properties of photosensitizers are one of the most important factors that influence the solar cell performance. Two outstanding Ru(II) polypyridyl sensitizers for nanocrystalline TiO2 solar cells so far reported are $[Ru(dcbpy)_2(NCS)_2\{(C_4H_9)_4N\}_2]$ and $[Ru(tctpy)(NCS)_3\{(C_4H_9)_4N\}_3]$, where dcbpy is 4,4′-dicarboxy-2,2′-bipyridine and tctpy is 4,4′,4″-tricarboxy-2,2′:6′,2″-terpyridine, yielding solar to electric power conversion efficiency of over 11% under standard AM 1.5 condition [5, 7–9]. To get an efficient solar cell performance, the sensitizer should fulfill several requirements, including that (i) the dye's absorption spectrum should overlap with the solar spectrum to get maximum power conversion, (ii) the excited state should have enough thermodynamic driving force for the injection of electrons into the conduction band, and (iii) the redox potential should be sufficiently positive so that the neutral sensitizer can be regenerated via electron donation from the redox electrolyte. Molecular design of new sensitizers for nanocrystalline TiO_2 solar cells that can absorb all solar radiation is a challenging task. The highest occupied molecular orbital (HOMO) and lowest unoccupied molecular orbital (LUMO) have to be maintained at the levels where photoinduced electron transfers into the TiO_2

conduction band. Moreover, the regeneration of the dye by iodide can take place practically at 100% yield is another challenge [10].

We have reported a series of ruthenium polypyridyl complexes where the LUMO energy level of the sensitizer is systematically tuned, and we show that a sensitizer should possess excited-state oxidation potential of −0.8 V versus SCE for efficient charge injection [11–17]. So far, terpyridine ruthenium(II) complex having one triphenylamine-substituted β-diketonato chelating ligand exhibits a broad absorption spectrum covering the visible and near-IR regions and a high molar extinction coefficient [14]. However, there is no report of systematic tuning of the HOMO energy level to elucidate the threshold ground-state redox potential for efficient dye regeneration. Thus we developed novel sensitizers, where we have systematically tuned the HOMO energy level by changing the electron donor ability of the β-diketonato ligands such as pentane-2,4-dione (pd), 3-methylpentane-2,4-dione (mepd), 2,2,6,6-tetramethylheptane-3,5-dione (tmhd), tridecane-6,8-dione (tdd), and 1,3-diphenylpropane-1,3-dione (dppd) compared to our previous complex [Ru(4,4′,4″-tricarboxy-2,2′:6′,2″-terpyridine)(1,1,1-trifluoropentane-2,4-dionato)(NCS)](**R1**) as a reference [13]. The molecular structures of the five new terpyridine-ruthenium(II) complexes [Ru(tctpy)(dppd)(NCS)] (**1**), [Ru(tctpy)(pd)(NCS)] (**2**), [Ru(tctpy)(tdd)(NCS)] (**3**), [Ru(tctpy)(mepd)(NCS)] (**4**), and [Ru(tctpy)(tmhd)(NCS)] (**5**) are shown in Figure 1. The photovoltaic performance and the threshold ground-state redox potential for efficient dye regeneration in DSCs are discussed.

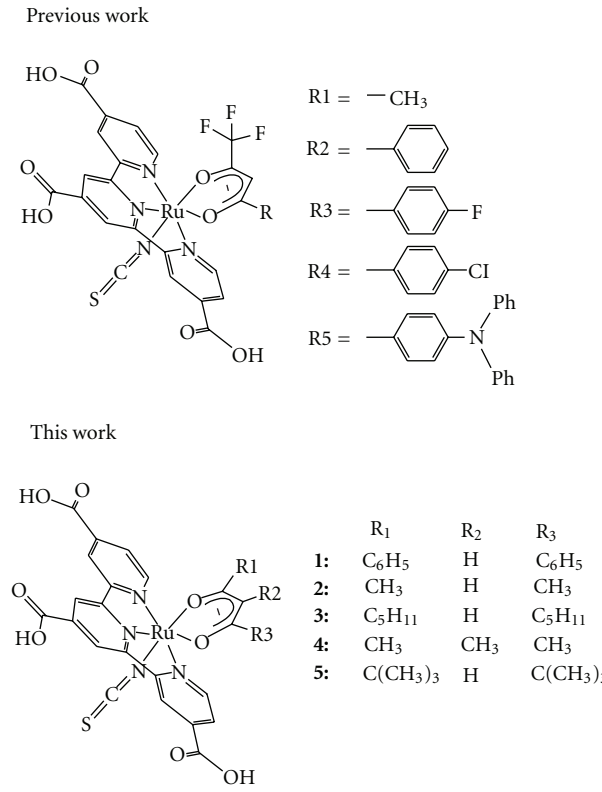

Figure 1: Molecular structures of complexes **1–5** (this work) and complexes R1–R5 (previous work).

2. Experimental Details

2.1. Materials. The following chemicals were purchased and used without further purification: hydrated ruthenium trichloride (from Aldrich), ammonium thiocyanate (from TCI), pentane-2,4-dione (pd), 3-methylpentane-2,4-dione (mepd), 2,2,6,6-tetramethylheptane-3,5-dione (tmhd), tridecane-6,8-dione (tdd), and 1,3-diphenylpropane-1,3-dione (dppd; from Aldrich). Solvents used in synthesis were of reagent grade. Chromatographic purification was performed by gel permeation on Sephadex LH-20 (from Sigma). Ru(4,4′,4″-trimethoxycarbonyl-2,2′:6′,2″-terpyridine)Cl_3 [7] was synthesized using literature procedures.

*2.1.1. Synthesis of [Ru(tctpy)(dppd)(NCS)] (**1**).* To a solution of complex Ru(4,4′,4″-trimethoxycarbonyl-2,2′:6′,2″-terpyridine)Cl_3 (307 mg, 0.5 mmol) in methanol (100 mL) were added dppd (448 mg, 2.0 mmol) and Et_3N (0.5 mL). The reaction mixture was refluxed for 8 h, and the solvent was allowed to evaporate on a rotary evaporator. The crude complex Ru(4,4′,4″-trimethoxycarbonyl-2,2′:6′,2″-terpyridine)(dppd)Cl was purified on a Sephadex LH-20 column using methanol as eluent. The green color band was collected and the solvent was allowed to evaporate on a rotary evaporator. The solid mass obtained was dissolved in 30 mL of DMF under nitrogen. To this solution 5 mL of an aqueous solution of NaSCN (300 mg, 3.7 mmol) was added. After refluxing for 8 h, 10 mL of Et_3N was added and the solution refluxed for a further 24 h to hydrolyze the ester groups on the terpyridine ligand. The reaction mixture was allowed to cool and the solvent volume reduced on a rotary evaporator to around 5 mL. Water was added to the flask and the insoluble solid was filtered and dried under vacuum. The complex Ru(tctpy)(dppd)(NCS) was further purified by loading onto a Sephadex LH-20 column with water as eluent. Yield 65%. MS (ESIMS): *m/z*: 248.2 $(M\text{-}3H)^{3-}$, 372.6 $(M\text{-}2H)^{2-}$. ^{1}H NMR (300 MHz, D_2O-NaOD): δ 8.56 (4H, s), 8.53 (2H, d), 8.02 (2H, d), 7.69 (2H, d), 7.51 (H, d), 7.41 (2H, t), 7.39 (H, t), 6.92 (4H, sm), 6.34 (H, s). Anal. Calcd for $C_{34}H_{22}N_4O_8SRu\cdot(H_2O)$: C, 53.33; H, 3.16; N, 7.32. Found: C, 53.03; H, 3.20; N, 7.40.

*2.1.2. Synthesis of [Ru(tctpy)(pd)(NCS)] (**2**).* Complex **2** was synthesized by the method used for **1** using ligand pentane-2,4-dione (pd). The title compound was obtained as a dark green powder. [Ru(tctpy)(pd)(NCS)] (**2**). Yield was 60%. MS (ESIMS): *m/z*: 206.7 $(M\text{-}3H)^{3-}$, 310.4 $(M\text{-}2H)^{2-}$. ^{1}H NMR (300 MHz, D_2O-NaOD): δ 8.59 (2H, s), 8.58 (2H, d), 8.51 (2H, d), 7.77 (2H, d), 5.45 (H, s), 2.31 (3H, s), 1.25 (3H, s)..Anal. Calcd for $C_{24}H_{18}N_4O_8SRu\cdot(H_2O)_2$: C, 43.70; H, 3.36; N, 8.49. Found: C, 43.20; H, 3.45; N, 8.50.

*2.1.3. Synthesis of [Ru(tctpy)(tdd)(NCS)] (**3**).* Complex **3** was synthesized by the method used for **1** using ligand tridecane-6,8-dione (tdd). The title compound was obtained as a dark

green powder. [Ru(tctpy)(tdd)(NCS){$(C_4H_9)_4N$}] (**3**). Yield was 56%. MS (ESIMS): *m*/*z*: 244.1 $(M\text{-}3H)^{3-}$, 367.4 $(M\text{-}2H)^{2-}$. ^{1}H NMR (300 MHz, D_2O-NaOD): δ 8.41 (4H, s), 8.31 (2H, d), 7.63 (2H, d), 5.21 (H, s), 2.33 (2H, t), 1.60 (2H, m), 1.29 (2H, t), 1.18 (4H, m), 0.65 (2H, t), 0.51 (3H, m), 0.38 (2H, m), 0.13 (2H, t), 0.02 (3H, m). Anal. Calcd for $C_{32}H_{35}N_4O_8SRu$: C, 52.17; H, 4.79; N, 7.60. Found: C, 51.85; H, 4.81; N, 7.85.

*2.1.4. Synthesis of [Ru(tctpy)(mepd)(NCS)] (**4**).* Complex **4** was synthesized by the method used for **1** using ligand 3-methylpentane-2,4-dione (mepd). The title compound was obtained as a dark green powder. [Ru(tctpy)(mepd)(NCS)] (**4**). Yield was 35%. MS (ESIMS): *m*/*z*: 211.8 $(M\text{-}3H)^{3-}$, 313.3 $(M\text{-}2H)^{2-}$.^{1}H NMR (300 MHz, D_2O-NaOD): δ 8.60 (2H, s), 8.58 (2H, d,), 7.78 (2H, d), 2.45 (3H, s), 1.78 (3H, s), 1.32 (3H, s). Anal. Calcd for $C_{25}H_{20}N_4O_8SRu$: C, 47.09; H, 3.16; N, 8.79. Found: C, 46.74; H, 3.23; N, 8.86.

*2.1.5. Synthesis of [Ru(tctpy)(tmhd)(NCS)] (**5**).* Complex **5** was synthesized by the method used for **1** using ligand 2,2,6,6-tetramethylheptane-3,5-dione (tmhd). The title compound was obtained as a dark green powder. [Ru(tctpy)(tmhd)(NCS)] (**5**). Yield was 55%. MS (ESIMS): *m*/*z*: 234.6 $(M\text{-}3H)^{3-}$, 352.7 $(M\text{-}2H)^{2-}$, 707.0 $(M\text{-}H)^{-}$.^{1}H NMR (300 MHz, D_2O-NaOD): δ 8.26 (4H, s), 8.13 (2H, d), 7.44 (2H, d), 5.40 (H, s), 1.03 (9H, s), 0.00 (9H, s). Anal. Calcd for $C_{30}H_{31}N_4O_8SRu \cdot (H_2O)$: C, 49.65; H, 4.44; N, 7.72. Found: C, 49.77 H, 4.62N, 7.89.

2.2. Spectroscopic Measurements. UV-visible spectra were recorded on a Shimadzu UV-3101PC spectrophotometer. Steady-state emission spectra were recorded using a grating monochromator (Triax 1900) and a CCD image sensor. The spectral sensitivity of the spectrophotometer was calibrated using a bromine lamp (Ushio IPD100 V 500 WCS). The emission lifetimes were measured by exciting the sample with a ~7 ns pulse at 500 nm from an optical parametric oscillator (Surelite OPO) pumped at 355 nm by a Nd : YAG laser (Continuum Surelite II). The emission decay was followed on a Tektronix TDS680C digitizing signal analyzer, having used a Hamamatsu R928 photomultiplier to convert the light signal to a voltage signal. Dewar vessel was used for the measurements at 77 K. ^{1}H NMR spectra were recorded by a Varian 300 BB spectrometer. Electrospray ionization mass spectra (ESIMS) were obtained on a Micromass Quattro II mass spectrometer.

2.3. Electrochemical Measurements. The redox potential of the complexes was measured using a standard three-electrode apparatus. The counter electrode was a platinum wire, the working electrode was a ruthenium-complex-adsorbed conducting nanocrystalline TiO_2 film, and the reference electrode was an Ag/AgCl (saturated aqueous KCl) in contact with a KCl salt bridge. Cyclic voltammograms were collected using an electrochemical analyzer. Scan rates were 0.05–0.5 Vs^{-1}. Acetonitrile was used as solvent and the supporting electrolyte was 0.1 M tetrabutylammonium perchlorate. Electrode potential values were calibrated to the saturated calomel electrode (SCE).

2.4. Preparation of TiO_2 Electrode. Nanocrystalline TiO_2 photoelectrodes of around 20 μm thickness (area: 0.25 cm^2) were prepared using a variation of a method reported by Nazeeruddin et al. [7]. Fluorine-doped tin oxide-coated glass electrodes (Nippon Sheet Glass Co., Japan) with a sheet resistance of 8–10 ohm^{-2} and an optical transmission of >80% in the visible range were used. Anatase TiO_2 colloids (particle size ~13 nm) were obtained from commercial sources (Ti-Nanoxide D/SP, Solaronix). The nanocrystalline TiO_2 thin films of approximately 20 μm thickness were deposited onto the conducting glass by screen-printing. The film was then sintered at 500°C for 1 h. The film thickness was measured with a Surfcom 1400 A surface profiler (Tokyo Seimitsu Co. Ltd.). The electrodes were impregnated with a 50 mM titanium tetrachloride solution and sintered at 500°C. The dye solutions (2×10^{-4} M) were prepared in 1 : 1 acetonitrile and *tert*-butyl alcohol solvents. Deoxycholic acid as a coadsorbent was added to the dye solution at a concentration of 20 mM. The electrodes were immersed in the dye solutions and then kept at 25°C for 20 h to adsorb the dye onto the TiO_2 surface.

2.5. Fabrication of Dye-Sensitized Solar Cell. Photovoltaic measurements were performed in a two-electrode sandwich cell configuration. The dye-deposited TiO_2 film was used as the working electrode, and a platinum-coated conducting glass was used as the counter electrode. Two electrodes were separated by a surlyn spacer (40 μm thick) and sealed up by heating the polymer frame. The electrolyte was composed of 0.6 M dimethylpropyl-imidazolium iodide (DMPII), 0.05 M I_2, and 0.1 M LiI in acetonitrile (AN).

2.6. Photovoltaic Characterization. The working electrode was illuminated through a conducting glass. The current-voltage characteristics were measured by using the previously reported method [18] with a solar simulator (AM-1.5, 100 mW/cm^2, WXS-155S-10: Wacom Denso Co. Japan). Monochromatic incident photon-to-current conversion efficiency (IPCE) for the solar cell, plotted as a function of excitation wavelength, was recorded on a CEP-2000 system (Bunkoh-Keiki Co. Ltd.). Incident photon-to-current conversion efficiency (IPCE) at each incident wavelength was calculated from (1), where I_{sc} is the photocurrent density at short circuit in mA cm^{-2} under monochromatic irradiation, q is the elementary charge, λ is the wavelength of incident radiation in nm, and P_0 is the incident radiative flux in W m^{-2}

$$\mathrm{IPCE}(\lambda) = 1240\left(\frac{I_{sc}}{q\lambda P_0}\right). \quad (1)$$

3. Results and Discussion

3.1. Photophysical Properties. The absorption, emission, and electrochemical properties of complexes **1–5** and reference

Table 1: Absorption, luminescence, and electrochemical properties of the ruthenium complexes.

Sensitizer	Absorption, [a]λ_{max}/nm ($\varepsilon/10^3$ M^{-1} cm^{-1})	Emission λ_{max} [b] /nm		Emission τ[b]/ns		E ($Ru^{3+/2+}$)[c]	E^*($Ru^{3+/2+}$)[d]
		298 K	77 K	298 K	77 K	/versus SCE	/versus SCE
1	294 (34.7), 329 (41.7), 440 (16.8), 615 (7.2)	990	930	13	225	+0.57	−0.89
2	293 (22.8) 330 (19.2), 433 (9.8), 622 (4.9)	995	950	11	170	+0.54	−0.89
3	293 (23.9), 331 (23.1), 438 (13.4), 629 (6.5)	1010	960	10	150	+0.53	−0.88
4	293 (32.0), 331 (18.7), 433 (12.2), 620 (5.5)	1010	960	8	147	+0.49	-0.91
5	293 (19.0), 332 (18.7), 435 (9.7), 630 (5.0)	1010	970	∼7	130	+0.46	−0.92
R1[e]	293 (27.6), 331 (22.7), 422 (14.7), 606 (7.0)	940		16		+0.68	

[a]Measured in 4 : 1 v/v ethanol:methanol at room temperature.
[b]The emission spectra and emission lifetime were obtained by exciting into the lowest MLCT band in 4 : 1 v/v ethanol:methanol.
[c]Half-wave potentials assigned to the $Ru^{3+/2+}$ couple for ruthenium sensitizers bound to nanocrystalline TiO_2 film, measured in 0.1 M $LiClO_4$ acetonitrile solution.
[d]Calculated from E^* ($Ru^{3+/2+}$) = E ($Ru^{3+/2+}$) − E^{0-0}; E^{0-0} values were estimated from the 5% intensity level of the emission spectra at 77 K.
[e]Data taken from [13].

complex [Ru(4,4′,4′′-tricarboxy-2,2′:6′,2′′-terpyridine)(1,1,1-trifluoropentane-2,4-dionato)(NCS)] (**R1**) are summarized in Table 1. The absorption spectra of complexes **1**, **3, 5,** and **R1** in ethanol-methanol solution are shown in Figure 2.The absorption spectra of the sensitizers **1–5** are dominated in the visible region by absorption between 433 and 630 nm, and in the UV region between 293 and 332 nm. The bands in the visible region are assigned to metal-to-ligand charge-transfer transitions (MLCT) and in the UV region to ligand π–π * transitions of 4,4′,4′′-tricarboxy-2,2′:6′,2′′-terpyridine [19]. In complexes **1–5**, the molar extinction coefficient of the lowest energy MLCT band shows in the range of 5000–7200 M^{-1} cm^{-1}. The low-energy MLCT absorption bands of complexes **1–5** are red-shifted from that of **R1** complex. The lower energy MLCT band maximum of complex **1** is observed at 615 nm, which is red-shifted by around 9 nm compared to that of complex **R1**. The molar absorption coefficient of this low-energy band is 7200 M^{-1} cm^{-1} and can absorb entire visible range of solar emission wavelengths. Substitution of the 1,1,1-trifluoropentane-2,4-dionato (tfac) ligand with the 1,3-diphenylpropane-1,3-dione (dppd) in complex **1** destabilizes the ground state by electron donation to Ru, causing an increase in the energy of the t_{2g} metal orbital compared to that of complex **R1** and thus red-shifts the lowest-energy MLCT band. When compared to the complex **1**, which shows a maximum at 615 nm, the lowest MLCT band of complex **5** is red-shifted by around 15 nm because of the stronger electron-donating nature of the methyl groups present in the 2,2,6,6-tetramethylheptane-3,5-dione ligand of complex **5**.

In this study, we have tuned the low-energy MLCT absorption band of the complexes **1–5** around 25 nm compared to **R1** with variation of the diketonato ligands having different electron-donating strengths (Table 1). The donor properties of the diketonato ligand decreases in the following order tmhd > mepd > pd ≈ tdd > dppd > tfac. In the red-light region, the diketonato complexes **1–5** show a distinct shoulder at around 720 nm, which is assigned to metal-to-ligand charge transfer (MLCT) transition (Figure 2) [20]. The enhanced red absorption of these complexes renders them attractive candidates as panchromatic charge transfer sensitizers for DSCs.

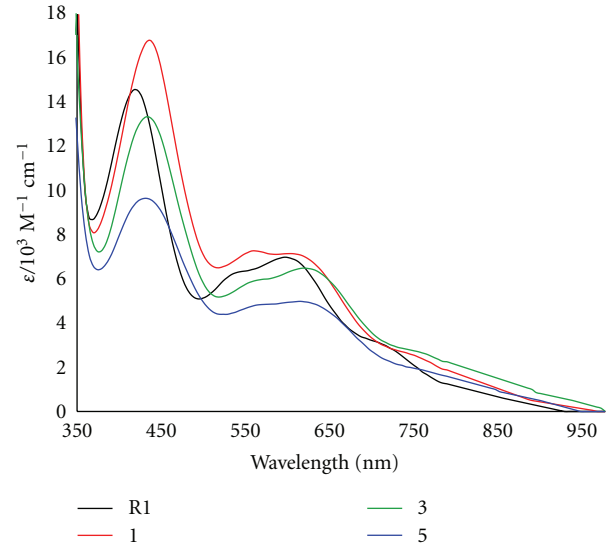

Figure 2: UV-vis absorption spectra of complexes **1**, **3**, **5**, and **R1** in ethanol-methanol (4 : 1) solution.

It is well known that the excited-state responsible for the luminescence of the Ru(II)-polypyridine compounds is the lowest-energy triplet metal-to-ligand charge-transfer (^{3}MLCT) state [21]. When excited at the charge transfer absorption band, complexes **1–5** show an intense emission at the 77 K ethanol-methanol glass matrix with a maximum between 930 and 970 nm. In degassed ethanol-methanol solution at 298 K, the emission spectra become weak and broad with a small shift to the lower-energy end. All complexes **1–5** show an emission at 298 K with a maximum between 990 nm and 1010 nm. The blue shift that occurs for all of the complexes in the transition from fluid solution to frozen solvent glass is a common rigidochromic effect observed in many metal diamine complexes [21, 22]. The emission spectra of complex **1** in ethanol-methanol mixed solvents at 77 and 298 K are presented in Figure 3. At 298 K,

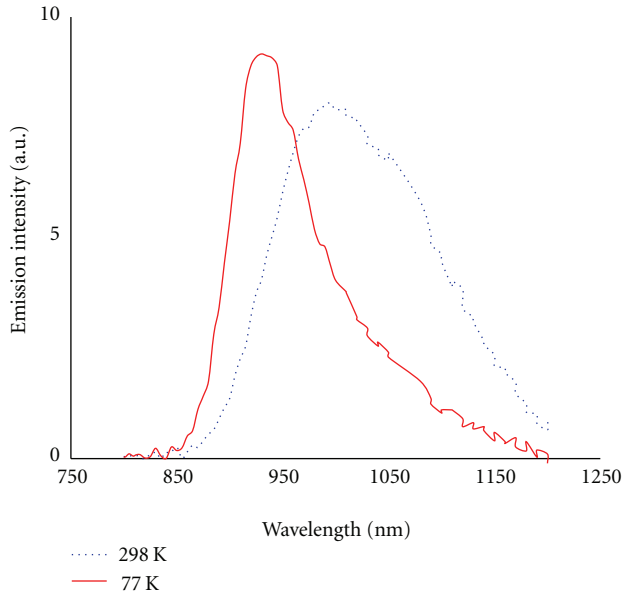

Figure 3: Emission spectra of complex **1** in ethanol-methanol (4 : 1) solution at 77 K (a) and 298 K (b).

complex **1** exhibits an emission maximum at 990 nm, which is 50 nm red-shifted compared to that of the **R1** emission and consistent with the shift in the lowest-MLCT absorption band. The luminescence data are gathered in Table 1. At 77 K, complexes **1–5** displayed excited-state lifetimes ranging from 225 to 130 ns. The lifetimes decrease significantly with the increase in temperature, to 7–13 ns in fluid solution at 298 K. The very short-lived excited state in fluid solution may be caused by efficient nonradiative decay via low-lying ligand-field excited states [21]. The excited-state lifetime of all the complexes is long enough for the process of electron injection into the conduction band of the TiO_2 electrode to make it efficient enough [23, 24]. To become a suitable sensitizer in DSCs, the band structure of the metal complex should match the conduction band of the semiconductor electrode and the redox potential of the electrolyte. The electrochemical data of the complexes measured in methanol solution are summarized in Table 1. All the complexes exhibit quasireversible oxidation wave for the $Ru^{3+/2+}$ couple ranging from +0.46 to +0.57 V versus SCE. The formation of an MLCT excited state of these complexes formally involves the oxidation of a HOMO having metal t_{2g} orbital character and reduction of a diimine-based LUMO. Table 1 shows that the ground-state oxidation potentials ($Ru^{3+/2+}$) of the β-diketonato complexes **1–5** are more negative than those of the complex **R1**. In these complexes, the energy of the acceptor orbital (LUMO) remains nearly constant and the decrease in MLCT transition energy arises mainly from the increase in the energy of the metal t_{2g} orbital (HOMO).

The excited-state oxidation potential, E^* ($Ru^{3+/2+}$), is a measure of the loss of the electron that is placed in the π^* (terpyridine) LUMO upon excitation. For complexes **1–5**, E^* ($Ru^{3+/2+}$) values are estimated using equation (2), where E ($Ru^{3+/2+}$) is the oxidation potential of the ground state and E^{0-0} is the energy difference between the lowest

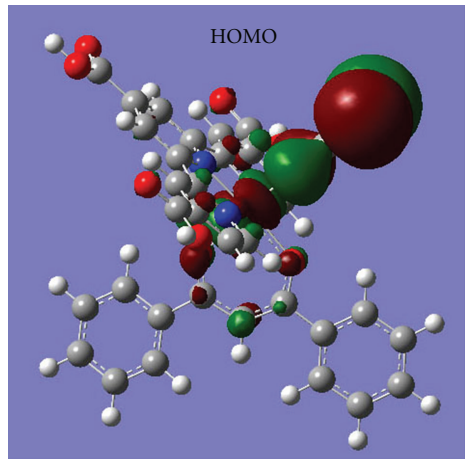

(a)

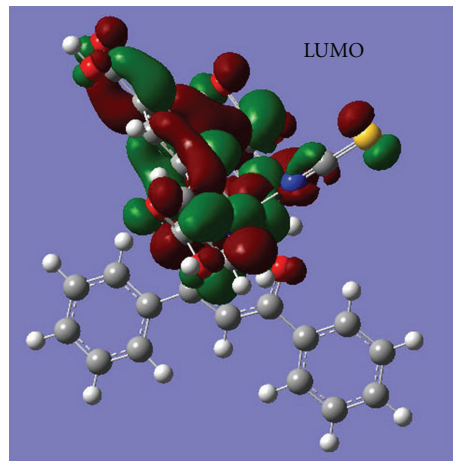

(b)

Figure 4: Graphic representation of the frontier molecular orbitals of complex **1**.

excited and ground states. The resulting E^* ($Ru^{3+/2+}$) values are shown in Table 1. The excited states of complexes **1–5** lie above the conduction band edge (–0.82 V versus SCE) of the nanocrystalline TiO_2 [2]. Efficient electron injection into the conduction band of the TiO_2 is thus possible for all of complexes **1–5**. The oxidation potential values of the complexes **1–5** lie above the I_3^-/I^- redox couple (0.07 V versus SCE) [25]

$$E^*\left(Ru^{3+/2+}\right) = E^*\left(Ru^{3+/2+}\right) - E^{0-0}. \quad (2)$$

To get an insight into the electron distribution of this new series of complexes for better understanding of the charge injection and dye regeneration process, the highest occupied molecular orbital (HOMO) and the lowest unoccupied molecular orbital (LUMO) of complex **1** were calculated by using Gaussian-03 program package (Figure 4). The HOMO of complex **1** is delocalized on Ru metal and NCS ligand, and the amplitude is primarily delocalized on the sulfur atom within the NCS ligand. The NCS group pointing in the direction of the electrolyte may facilitate reduction of the oxidized dye (Ru^{3+}) through reaction with

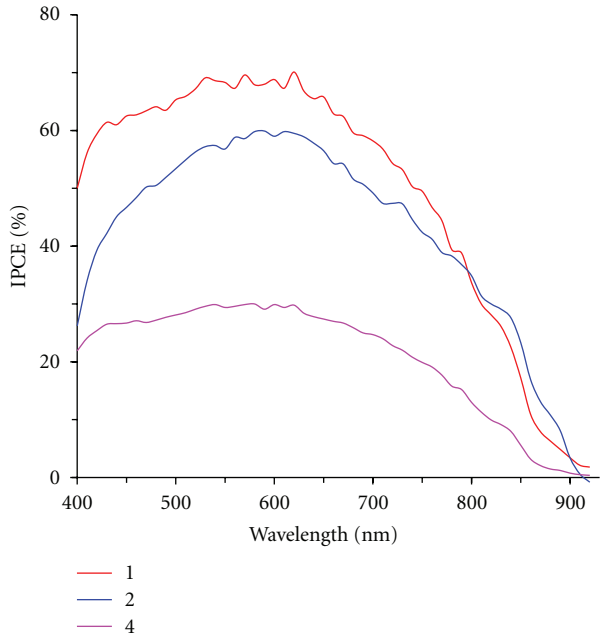

Figure 5: Photocurrent action spectra obtained with complexes **1** (a), **2** (b), and **4** (c) attached to nanocrystalline TiO_2 film. The incident photon-to-current conversion efficiency is plotted as a function of wavelength. A sandwich type sealed cell configuration was used to measure this spectrum. The electrolyte composition was 0.6 M DMPII, 0.05 M I_2, and 0.1 M LiI in acetonitrile.

I^-. The β-diketonato ligand has a negligible contribution to HOMO. The LUMO has homogeneous amplitudes on the terpyridine ligand, facilitating the electron injection from the photoexcited sensitizer to the TiO_2 semiconductor.

3.2. Photovoltaic Properties. The photovoltaic performance of complexes **1–5** on nanocrystalline TiO_2 electrode was studied under standard AM 1.5 irradiation (100 mW cm^{-2}) using an electrolyte with a composition of 0.6 M dimethylpropyl-imidazolium iodide (DMPII), 0.05 M I_2, and 0.1 M LiI in acetonitrile. Figure 5 shows the photocurrent action spectra for complexes **1**, **2**, and **4** where the incident photon to current conversion efficiency (IPCE) values is plotted as a function of wavelength. The maximum IPCE values of complexes **1–5** are listed in Table 2. Complexes **1–3** achieved efficient sensitization of nanocrystalline TiO_2 over the whole visible range extending into the near IR region. The most efficient sensitizer in this series was complex **1** that shows an IPCE value of 70% in the plateau region. Taking into account the reflection and absorption losses by the conducting glass, the photon-to-current conversion efficiency in this range reaches around 85%. One of the possible explanations for this low IPCE value of complex **1** is the aggregation of sensitizer molecules on TiO_2 surface. The red response was improved by replacing dppd with tdd while injection efficiencies were very low throughout the visible region (Figure 5). The maximum IPCE values of these β-diketonato complexes **1–5** decreases with the decrease in the ground-state oxidation potentials ($Ru^{3+/2+}$) values. Complexes **4** and **5** showed a drastically reduced IPCE value

Table 2: Photovoltaic properties of ruthenium polypyridyl sensitizers[a].

Sensitizer	$IPCE_{max}$	J_{sc} (mA cm^{-2})	V_{oc} (V)	FF	η (%)
1	70	16.7	0.58	0.64	6.2
2	61	14.2	0.57	0.66	5.3
3	54	13.0	0.58	0.70	5.3
4	30	7.6	0.56	0.70	3.0
5	24	6.2	0.45	0.71	2.0
R1[b]	70	18.3	0.57	0.64	6.7

[a] Conditions: sealed cells; coadsorbate, DCA 40 mM; photoelectrode, TiO_2 (20 μm thickness and 0.25 cm^2); electrolyte, 0.6 M DMPII, 0.1 M LiI, 0.05 I_2 in AN; irradiated light, AM 1.5 solar light (100 mW cm^{-2}). J_{sc}, short-circuit photocurrent density; V_{oc}, open-circuit photovoltage; FF, fill factor; η, total power conversion efficiency; IPCE, incident photon-to-current conversion efficiency.
[b] Data taken from [13].

(i.e., <30%) in the plateau region, and this reduction may be due to the decrease in the dye regeneration rate after tuning the ground-state oxidation potential toward more negative range. The recombination rate of injected electrons with the oxidized dye is an important factor that affects the electron collection efficiency. The recombination rates will increase by changing the oxidation values toward more negative potential. After electron injection, a competition is setup between charge recombination and iodide oxidation by oxidized dye. Considering the relative driving force of these complexes, the charge recombination rates will increase in the order of **1** < **2** ≈ **3** <**4** ≈ **5**. The low injection efficiencies ($IPCE_{max}$ = 24–30%) of the complexes **4-5** compared to the complexes **1–3** can be explained by the fact that these complexes have more negative $Ru^{3+/2+}$ ground state oxidation potential compared to those of the complexes **1–3** and the back reaction of injected electrons with Ru(III) competes to regeneration of Ru(II) through reaction with iodide. The ground-state potential of complex **3** (+0.53 V versus SCE) offers a minimum limit for the ground-state redox potential of the dye in the current configuration of the electrochemical cell and redox couple.

Figure 6 shows the photocurrent-voltage curves obtained under AM1.5 simulated illumination of the various dye coated TiO_2 electrode systems studied in this work. The short-circuit photocurrent density (J_{sc}), open-circuit voltage (V_{oc}), fill factors (FF), and overall cell efficiencies (η) for each dye-TiO_2 electrode are summarized in Table 2. The dppd complex **1** shows the best performance in this series. The solar cell sensitized with complex **1** showed a photocurrent density of 16.7 mA cm^{-2}, an open circuit potential of 0.58 V, and a fill factor of 0.64, corresponding to an overall conversion efficiency (η) of 6.2%. The complexes **4-5** showed poor cell performance (η < 3%) compare to those of complexes **1–3.** The low injection efficiencies ($IPCE_{max}$ = 24–30%) of complexes **4-5** decrease the short-circuit photocurrent density (J_{sc}), and thus the decrease of overall cell efficiencies.

Thus, this class of diketonato ruthenium complexes serves as a basis for further design of new potential sensitizers by introducing suitable substituents on the diketonato ligand

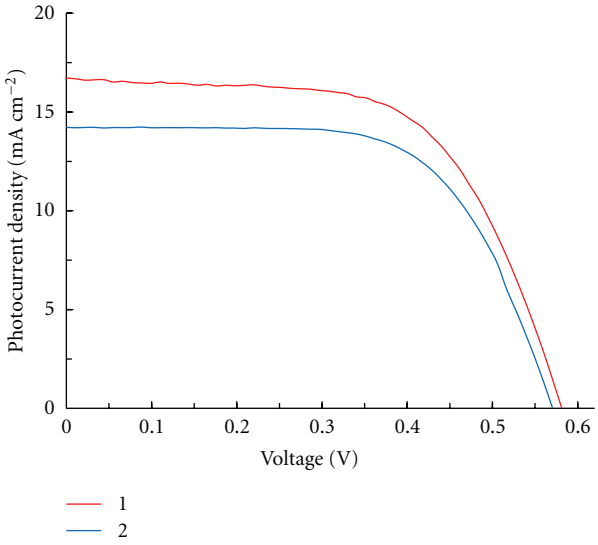

Figure 6: Photocurrent voltage characteristics of DSCs sensitized with the complexes **1** (a) and **2** (b) at AM 1.5 illuminations (light intensities: 100 mW cm^{-2}. The redox electrolyte consisted of a solution of 0.6 M DMPII, 0.05 M I_2, and 0.1 M LiI in acetonitrile.

to adjust a desired electronic environment on the metal center for efficient dye regeneration. Since the modifications of electronic and steric environments in the sensitizing molecules are possible by changing the substituents on the diketonate ligand, further improvement in the solar cell efficiency will be accomplished in the near future.

4. Conclusions

Five new panchromatic photosensitizers based on 4,4′,4″-tricarboxy-2,2′:6′,2″-terpyridine -ruthenium(II) complexes with one β-diketonato chelating ligand, pentane-2,4-dione (pd), 3-methylpentane-2,4-dione (mepd), 2,2,6,6-tetramethylheptane-3,5-dione (tmhd), tridecane-6,8-dione (tdd), or 1,3-diphenylpropane-1,3-dione (dppd) were developed, and systematically characterized using electrochemical and spectroscopic methods. The low-energy MLCT transitions in these complexes have been tuned by increasing the donor strength of the β-diketonato ligand to extend the spectral response of nanocrystalline TiO_2 electrodes to a range of longer wavelengths. The decrease in MLCT transition energy arises mainly from the negative shift in the ground state oxidation potential, that is, the energy of the metal t_{2g} orbital (HOMO).The complexes achieved efficient sensitization of nanocrystalline TiO_2 over the whole visible range extending into the near IR region (ca. 950 nm). The photovoltaic data of these new complexes shows 6.2% power conversion efficiency under standard AM 1.5 irradiation (100 mW cm^{-2}). Though complexes **4** and **5** have superior panchromatic light-harvesting properties compared to the complex **1**, they show poor overall photovoltaic performance. A sluggish halide oxidation rate and a fast recombination of injected electron with the oxidized dye due to unfavorable HOMO energy level are perhaps responsible for the low cell efficiency of these complexes.

References

[1] B. O'Regan and M. Grätzel, "A low-cost, high-efficiency solar cell based on dye-sensitized colloidal TiO_2 films," *Nature*, vol. 353, no. 6346, pp. 737–740, 1991.

[2] A. Hagfeld and M. Grätzel, "Light-induced redox reactions in nanocrystalline systems," *Chemical Reviews*, vol. 95, no. 1, pp. 49–68, 1995.

[3] M. Grätzel, "Conversion of sunlight to electric power by nanocrystalline dye-sensitized solar cells," *Journal of Photochemistry and Photobiology A*, vol. 164, no. 1–3, pp. 3–14, 2004.

[4] A. Hagfeldt and M. Grätzel, "Molecular photovoltaics," *Accounts of Chemical Research*, vol. 33, no. 5, pp. 269–277, 2000.

[5] M. K. Nazeeruddin, A. Kay, I. Rodicio et al., "Conversion of light to electricity by *cis*-X_2bis(2,2′-bipyridyl-4,4′-dicarboxylate)ruthenium(II) charge-transfer sensitizers (X = Cl^-, Br^-, I^-, CN^-, and SCN^-) on nanocrystalline TiO_2 electrodes," *Journal of the American Chemical Society*, vol. 115, no. 14, pp. 6382–6390, 1993.

[6] K. Hara, H. Sugihara, Y. Tachibana et al., "Dye-sensitized nanocrystalline TiO_2 solar cells based on ruthenium(II) phenanthroline complex photosensitizers," *Langmuir*, vol. 17, no. 19, pp. 5992–5999, 2001.

[7] M. K. Nazeeruddin, P. Péchy, T. Renouard et al., "Engineering of efficient panchromatic sensitizers for nanocrystalline TiO_2-based solar cells," *Journal of the American Chemical Society*, vol. 123, no. 8, pp. 1613–1624, 2001.

[8] M. K. Nazeeruddin, F. D. Angelis, S. Fantacci et al., "Combined experimental and DFT-TDDFT computational study of photoelectrochemical cell ruthenium sensitizers," *Journal of the American Chemical Society*, vol. 127, no. 48, pp. 16835–16847, 2005.

[9] Y. Chiba, A. Islam, Y. Watanabe, R. Komiya, N. Koide, and L. Han, "Dye-sensitized solar cells with conversion efficiency of 11.1%," *Japanese Journal of Applied Physics*, vol. 45, no. 25, pp. L638–L640, 2006.

[10] A. Islam, H. Sugihara, and H. Arakawa, "Molecular design of ruthenium(II) polypyridyl photosensitizers for efficient nanocrystalline TiO_2 solar cells," *Journal of Photochemistry and Photobiology A*, vol. 158, no. 2–3, pp. 131–138, 2003.

[11] A. Islam, F. A. Chowdhury, Y. Chiba et al., "Synthesis and characterization of new efficient tricarboxyterpyridyl (β-diketonato) ruthenium(II) sensitizers and their applications in dye-sensitized solar cells," *Chemistry of Materials*, vol. 18, no. 22, pp. 5178–5185, 2006.

[12] A. Islam, F. A. Chowdhury, Y. Chiba et al., "Ruthenium(II) tricarboxyterpyridyl complex with a fluorine-substituted β-diketonato ligand for highly efficient dye-sensitized solar cells," *Chemistry Letters*, vol. 34, no. 3, pp. 344–345, 2005.

[13] A. Islam, H. Sugihara, M. Yanagida et al., "Efficient panchromatic sensitization of nanocrystalline TiO_2 films by β-diketonato ruthenium polypyridyl complexes," *New Journal of Chemistry*, vol. 26, no. 8, pp. 966–968, 2002.

[14] S. Gao, A. Islam, Y. Numata, and L. Han, "A β-diketonato ruthenium(II) complex with high molar extinction coefficient for panchromatic sensitization of nanocrystalline TiO_2 film," *Applied Physics Express*, vol. 3, no. 6, Article ID 062301, 3 pages, 2010.

[15] S. P. Singh, A. Islam, M. Yanagida, and L. Han, "Development of a new class of thiocyanate-free cyclometallated ruthenium(II) complex for sensitizing nanocrystalline TiO_2 solar cells," *International Journal of Photoenergy*, vol. 2011, p. 5, 2011.

[16] A. Islam, S. P. Singh, M. Yanagida, R. Karim, and L. Han, "Amphiphilic ruthenium(II) terpyridine sensitizers with long alkyl chain substituted β-diketonato ligands: An efficient coadsorbent free dye-sensitized solar cells," *International Journal of Photoenergy*, vol. 2011, p. 7, 2011.

[17] A. Islam, S. P. Singh, and L. Han, "Thiocyanate-free, panchromatic ruthenium(II) terpyridine sensitizer having a tridentate diethylenetriamine ligand for near-IR sensitization of nanocrystalline TiO_2," *Functional Materials Letters*, vol. 4, no. 1, pp. 21–24, 2011.

[18] N. Koide and L. Han, "Measuring methods of cell performance of dye-sensitized solar cells," *Review of Scientific Instruments*, vol. 75, no. 9, pp. 2828–2831, 2004.

[19] A. Mamo, A. Juris, G. Calogero, and S. Campagna, "Near-infrared luminescence at room temperature of two new osmium(II) terdentate polypyridine complexes," *Chemical Communications*, no. 10, pp. 1225–1226, 1996.

[20] Y. Takahashi, H. Arakawa, H. Sugihara et al., "Highly efficient polypyridyl-ruthenium(II) photosensitizers with chelating oxygen donor ligands: β-diketonato-bis(dicarboxybi-pyridine)ruthenium," *Inorganica Chimica Acta*, vol. 310, no. 2, pp. 169–174, 2000.

[21] A. Islam, N. Ikeda, A. Yoshimura, and T. Ohno, "Nonradiative transition of phosphorescent charge-transfer states of ruthenium(II)-to-2, 2′-biquinoline and ruthenium(II)-to-2, 2′ : 6′, 2″-terpyridine in the solid state," *Inorganic Chemistry*, vol. 37, no. 12, pp. 3093–3098, 1998.

[22] A. Juris, V. Balzani, F. Barigelletti, S. Campagna, P. Belser, and A. Zelewsky, "Ru(II) polypyridine complexes: photophysics, photochemistry, eletrochemistry, and chemiluminescence," *Coordination Chemistry Reviews*, vol. 84, no. C, pp. 85–277, 1988.

[23] Y. Tachibana, S. A. Haque, I. P. Mercer, J. R. Durrant, and D. R. Klug, "Electron injection and recombination in dye sensitized nanocrystalline titanium dioxide films: a comparison of ruthenium bipyridyl and porphyrin sensitizer dyes," *Journal of Physical Chemistry B*, vol. 104, no. 6, pp. 1198–1205, 2000.

[24] J. M. Rehm, G. L. McLendon, Y. Nagasawa, K. Yoshihara, J. Moser, and M. Grätzel, "Femtosecond electron-transfer dynamics at a sensitizing dye-semiconductor (TiO_2) interface," *Journal of Physical Chemistry*, vol. 100, no. 23, pp. 9577–9578, 1996.

[25] G. Oskam, B. V. Bergeron, G. J. Meyer, and P. C. Searson, "Pseudohalogens for dye-sensitized TiO_2 photoelectrochemical cells," *Journal of Physical Chemistry B*, vol. 105, no. 29, pp. 6867–6873, 2001.